NASA TECHNICAL NOTE

NASA TN D-2752

NASA TN D-2752
c. 1

A VERTICAL TEST RANGE FOR ANTENNA RADIATION MEASUREMENTS

by John Steckel and William Korvin

Goddard Space Flight Center
Greenbelt, Md.

NATIONAL AERONAUTICS AND SPACE ADMINISTRATION • WASHINGTON, D. C. • APRIL 1965

NASA TN D-2752

A VERTICAL TEST RANGE FOR ANTENNA RADIATION MEASUREMENTS

By John Steckel and William Korvin

Goddard Space Flight Center
Greenbelt, Md.

NATIONAL AERONAUTICS AND SPACE ADMINISTRATION

For sale by the Clearinghouse for Federal Scientific and Technical Information
Springfield, Virginia 22151 – Price $2.00

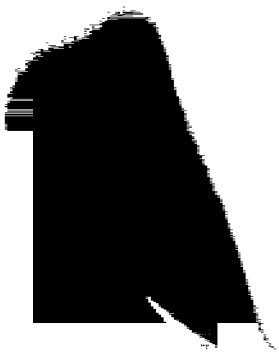

A VERTICAL TEST RANGE FOR ANTENNA RADIATION MEASUREMENTS

by
John Steckel and William Korvin
Goddard Space Flight Center

SUMMARY

In order to facilitate the measuring of satellite antenna radiation patterns in a controlled RF environment, the "Vertical RF Test Range", an anechoic chamber for VHF radio waves, was devised. Of primary importance was the capability to absorb and/or suppress undesirable electromagnetic energy at frequencies as low as 125 Mc, which would normally be reflected by the chamber floor and walls. The satellite antennas of concern are of the broad-pattern, near-omnidirectional type. The preliminary study and scale model measurements indicated that a reflection coefficient of 20-25 db can be expected in an electrically small chamber of $1\lambda \times 2\lambda \times 2\lambda$. Subsequent full-scale measurements have verified this. It was anticipated that the reflected energy level would decrease as the test frequency was raised, and this was borne out by scale model measurements. The dominant controlling factor at high frequencies is the structural weather protective radome. At the lowest frequency (125 Mc), the radome appears as a thin wall (about 0.05λ thick), but as the frequency is increased, the radome thickness becomes increasingly significant.

CONTENTS

A VERTICAL TEST RANGE FOR ANTENNA RADIATION MEASUREMENTS

by
John Steckel and William Korvin
Goddard Space Flight Center

INTRODUCTION

Antenna Test Range

The most important feature of an antenna test range is the control and reduction of reflections to the extent that they do not introduce significant errors in the measurement of the system under test. Because of this, most test range sites are chosen in open fields clear of reflecting objects. Satisfactory operation is obtained when the system under test is sufficiently directive to discriminate against reflections from the ground and the test tower. Antennas for small scientific spacecraft are operated in the UHF region and designed to be as nearly omnidirectional as possible, and thus are a "worst case" for conventional test ranges. The ideal solution is to provide a reflectionless environment that still permits convenient operation of the system under test.

One approach to this solution is the vertical test range shown in Figure 1, which uses an anechoic chamber as one terminal of the range. Recent advances in RF absorbent material have improved the performance of RF anechoic chambers to the point where they are comparable with the best outdoor range sites.

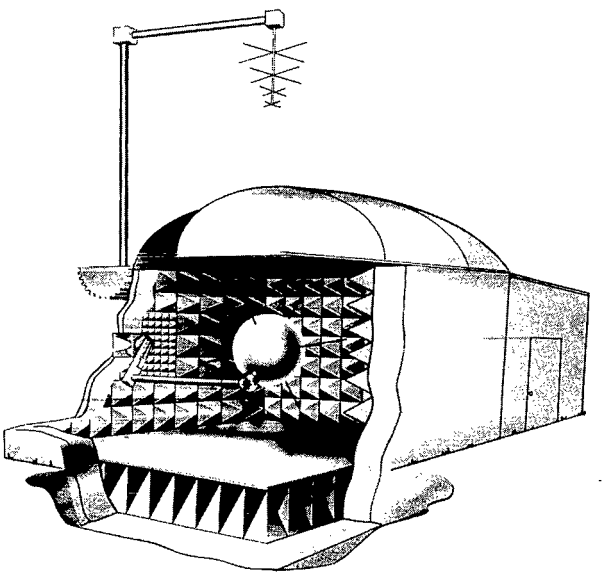

Figure 1—Vertical test range.

Definition of RF Anechoic Chamber

An RF anechoic chamber may be defined as an enclosure, suitably lined with an electromagnetic energy suppressing (absorbing and scattering) material, which may be used to measure such electrical characteristics as impedance, radiation pattern, and back-scatter of a body within the chamber. Further, the degree of suppression of undesirable electromagnetic reflections must approximate free space. The

allowable departure from free space is a function of the type of test and the tolerable error which the designer places on the test. For instance, a higher level of reflections may be tolerable when measuring impedance than when attempting back-scattering measurements.

Testing Criteria as a Function of Type of Test: Impedance, Back-Scatter, and Radiation Pattern

A primary requirement for measuring "free space" impedance of an antenna is the exclusion of all external sources of reflection. This requirement at first appears extremely stringent, if not impossible: to meet it rigorously would require that the impedance measurements be made miles from the earth's surface and from within the antenna system. Fortunately, the requirement can be relaxed to a degree governed by the tolerable error permitted in the system impedance expressed as a voltage standing wave ratio (VSWR). Consider a perfectly matched antenna system radiating energy. Under a condition of no electrical mismatch from external sources there would be no standing wave and the VSWR would be 1.00:1. In practice, all antenna systems exhibit some mismatch from reflections due to electrical discontinuities. The vector addition of the incident and reflected voltages results in a standing wave, the magnitude of which is expressed in the familiar form:

$$VSWR_{db} = 20 \log_{10} \frac{E_1}{E_2} \tag{1}$$

when

E_1 = incident voltage,

E_2 = reflected voltage.

This VSWR is an indication of the power transfer of an antenna system. For instance, a system with a VSWR of 6:1 would reflect 1/2 of the available power, which is intolerable in most applications. Table 1 indicates the percentage of RF power transmitted as a function of the system VSWR .

Table 1

RF Power Versus System VSWR

VSWR	RF Power Transmitted
1.00:1	100%
1.04:1	99.96%
1.22:1	99.02%
6.0:1	50%

Since a perfect impedance match is seldom achieved, the question then becomes one of how large a reflection due to the test site environment is tolerable, while still permitting measurement of the system impedance with reasonable accuracy. Consider first a worst case condition: all the incident energy striking a reflecting surface is reflected back to the antenna under test. If the power P_0 radiated from a perfectly

matched antenna of unity gain travels a distance R to a reflecting wall and is completely reflected back to the antenna, a standing wave will result. However, inverse square attenuation of the reflected electromagnetic wave will reduce its amplitude so that the VSWR induced will be less than infinite. For example, the attenuation of a 136 Mc signal to a reflecting wall 8 feet away can be computed from:

$$\alpha = 37 + 20 \log f + 20 \log R \ , \tag{2}$$

where

α = attenuation (db) ,

f = frequency (Mc) ,

R = distance (feet) ;

then

$$\alpha = 23.53 \text{ db} \ .$$

Assuming perfect reflection from the wall, the signal will be further reduced by 6 db in the return path to the antenna. Thus, the returned signal will be about 29.5 db below the incident signal. The resulting mismatch to the perfectly matched antenna is computed from:

$$|\Gamma| = \frac{r - 1}{r + 1} \ , \tag{3}$$

where

$|\Gamma|$ = reflection coefficient = .0335 .

Thus

$$r = \text{VSWR} = 1.07:1 \ .$$

The impedance of a low gain antenna system may thus be measured with confidence if the walls of the enclosure are at least eight feet away and are less effective as a reflector than a metallic wall. The requirement on the absorption of unwanted reflections from the environment is then easily met when making impedance or VSWR measurements on low gain antenna systems.

By definition, σ , the scattering cross section of a body, is the ratio of the power scattered per unit solid angle to the power incident per unit area. In terms of the radar equation,

$$\sigma = \frac{P_R 16\pi^2 R^4}{P_T G_T G_R \lambda^2} \text{ square meters} , \quad (4)$$

where

λ = the wavelength in meters,
R = the distance between the source antenna and the scattering cross section body in meters,
P_T = the transmitted RF power,
P_R = the received (reflected) RF power,
G_T = the transmitting antenna power gain with respect to an isotropic radiator,*
G_R = the receiving antenna power gain with respect to an isotropic radiator.*

The problem of measuring scattering cross sections in an anechoic chamber is therefore the suppression of the energy reflected from the chamber walls back to a receiving antenna. The necessary chamber performance, as in the case of VSWR measurements in a chamber, is relative. For example, a large scattering cross section would reflect an energy level which could be many orders of magnitude greater than energy contributed by the reflected energy from the chamber walls (including ceiling). In this case a percentage tolerance error can be established. Unfortunately, many radar cross section measurements are made of objects which have a small scattering cross section. Now, although the walls of the chamber absorb and suppress the RF energy, the fact that the walls are many orders of magnitude in size larger than the object being measured results in a chamber wall reflection coefficient which is as large as or larger than the object to be measured. In other words, the scattering energy of the body to be measured is hidden by the reflections from the chamber.

One technique which is described by Elery F. Buckley (Reference 1) allows a calibration of a chamber for measuring radar cross sections in a controlled manner. A transmitting and receiving antenna are placed at one end of a chamber. Two or more conducting spheres of known and differing physical size (and hence known and differing radar cross section) are placed at the opposite end of the chamber one at a time. Each sphere is rotated eccentrically about an axis, producing a phase response proportional to the amount of rotation. There will be two amplitude components for each sphere contributing to the recorded interference pattern. One component is from the sphere; the other is the constant field which is equal to the energy return from the chamber plus the electric field from transmitter-receiver cross coupling. The voltage ratio of these components produces an ambiguity—the chamber scattering cross section will be either of two values. For this reason the second measurement is made using a different conducting sphere with a known σ. The second measurement also yields two values for the chamber cross section, and the true chamber reflecting cross section is that cross section which is common to both measurements.

*An isotropic radiator is a fictitious antenna, used as a reference, which radiates energy truly omnidirectionally. Further, assuming this antenna is radiating an RF power of one watt, the magnitude of the electric field strength measured at a radius of 1 mile from the source is equal to 3.40mw/meter.

An example which illustrates the magnitude of energy suppression that an anechoic chamber must exhibit for the measurement of radar cross sections follows:

Let the scattering cross section be that produced by a sphere of radius $a = 0.1$ meter when $\lambda = 3$ cm (i.e., $a/\lambda > 1$). Then the scattering cross section is

$$\sigma_1 = \pi a^2 = 3.14 \times 10^{-2} \text{ meter}^2 \qquad (5)$$

Now, the return power received by an antenna G_r from a scattering body of cross section σ when the transmitted power P_T is radiated by an antenna G_T is

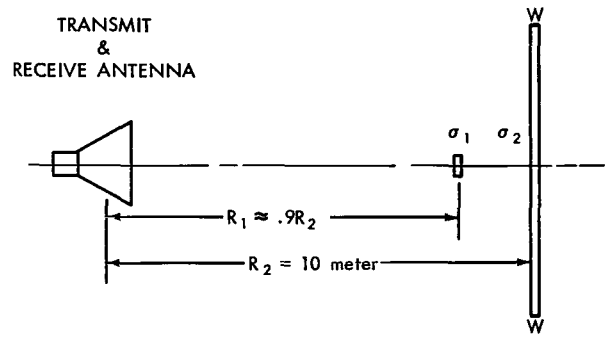

Figure 2—Measurement of scattering cross-section.

$$P_R = \frac{P_T G_R G_T \lambda^2}{16\pi^2 R^4} \sigma \quad . \qquad (6)$$

Consider first the return power received from the spherical scattering body and letting $P_T = 1$ watt, $R_1 = 9$ meters, so that

$$G_T = G_R = 63 \text{ and } \lambda = 3 \text{ cm} \quad .$$

Then

$$P_{R_1} = \frac{P_T G_R G_T \lambda^2}{16\pi^2 R^4} \sigma_1 \quad , \qquad (7)$$

and

$$P_{R_1} = 0.109 \times 10^{-6} \text{ watts} \quad .$$

Next, assume the wall W-W in Figure 2 to be a perfectly reflecting surface 3 meters on a side so that the wall radar cross section is

$$\sigma_2 = \frac{4\pi A^2}{\lambda^2} \quad , \qquad (8)$$

where A = wall area and λ = wavelength at the operating frequency. Then,

$$\sigma_2 = 12.56 \times 10^4 \text{ m}^2 \quad .$$

The return power received from the back wall W-W is (neglecting the small effect of the side, top and bottom walls)

$$P_{R_2} = \frac{P_T\ G_R\ G_T\ \lambda^2}{16\pi^2\ R^4}\ \sigma_2 \tag{9}$$

and

$$P_{R_2} = 0.284 \text{ watts}$$

By comparison,

$$\frac{P_{R_1}}{P_{R_2}} = -64.2 \text{ db} , \tag{10}$$

and from this it may be seen that the energy normal to the back wall W-W must be suppressed by 64.2 db to allow the spherical body (.1 meter radius) to present an equal amplitude to the receiver antenna G_R. Further suppression of the back wall energy must be attained before the energy from the spherical body is discernible above the energy scattered from the back wall.

The example outlined above now allows a feeling for the nature and magnitude of energy suppression and/or absorbing characteristics that may be required of an RF anechoic chamber designed to measure radar cross sections.

Measurement of antenna radiation patterns generally requires a better anechoic chamber than one for the measurement of antenna impedance. The requirements, however, are not as critical as for radar cross section (back-scatter) measurements. As an illustration, let us examine a typical E-plane pattern of a horn antenna and then show the effects of various magnitudes of reflected energy interfering at various aspect angles in the chamber. Figure 3 shows the E-plane pattern as measured in a controlled environment at an outside antenna range. The pattern approaches the theoretical pattern for a horn antenna exhibiting uniform distribution across the aperture. Figure 3 also shows a ray outline of reflected energy when measuring the E-plane pattern of this antenna in an anechoic chamber. Let sources of reflection be located at angles defined by $\theta = 50°$ and $60°$. Then the resulting perturbations from these reflecting sources are shown in Figure 3 as dashed curves. The deviations in the pattern are identified as ① , ② , and ③ . The magnitude of the perturbation at ① is 1.6 db. The magnitude of the reflected energy from point ① which produces this 1.6 db perturbation is equal to 21 db since the reflection coefficient in db is:

$$20 \log \frac{S - 1}{S + 1} \tag{11}$$

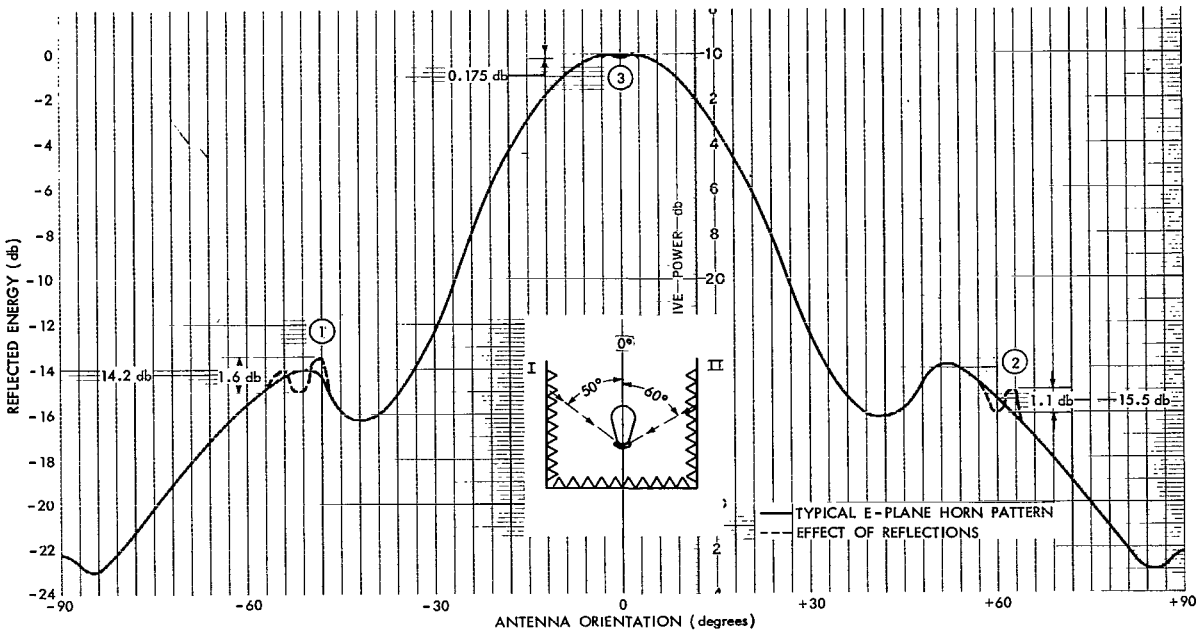

Figure 3—Effect of reflected energy on typical E-plane pattern of horn antenna.

where S = standing wave ratio. Referring to the figure, it can be seen that the perturbations take place at a level of -14.2 db on the radiation pattern. Therefore, the actual reflection coefficient (magnitude of the interfering reflected energy) is 35.2 db. At point ② the deviation from point ② is 1.1 db, corresponding to a reflection coefficient of 25 db. Since the radiated energy is down 15.5 db at this point, the actual reflection coefficient is 40.5 db. Now consider point ③ (i. e., 0 db down on the pattern). A reflection coefficient of 40 db will cause a perturbation of 0.175 db in the pattern at this point.

One can now see clearly the effect of reflected energy on a typical pattern from arbitrarily chosen points in an anechoic chamber enclosure which is 35 db to 40 db down from the incident energy.

DESCRIPTION OF VERTICAL RF TEST RANGE

Physical Description

The walls and floor of the vertical test range (Figure 1) are made of reinforced concrete. Attached to the chamber through a common wall is the control room, which houses all the electrical measuring devices. Opposite the control room side are two doors which, when opened, allow the chamber to be used as one end of a horizontal antenna range (in conjunction with available antenna towers). The roof of the chamber is an A-sandwich type RF transparent radome. Also shown in this figure are the outside azimuth - elevation mount for the source antenna. It has a fiberglass mast

approximately 35 feet high, which is controlled from inside, and facilitates the changing of source antennas. Inside the chamber (see Figure 4) is a wall-mounted rotating offset antenna mount which allows measurement of a satellite antenna system at or near the center of the chamber quiet zone.

The walls are lined with pyramidal absorbent foam, 70 inches in height and 2 feet square at the base (Figure 5). In the area of the side wall mount smaller pyramidal absorbent material is used, allowing the rotation of the offset rotating mount. The floor of the chamber is lined with 70 inch foam pyramids on top of which is cemented a smooth deck of 1/2"-thick sheets of semi-rigid vinyl foam which will support a man's weight during the setting up of experiments within the chamber. This allows an available working space inside the chamber of 14 feet by 10 feet in height.

The radome is a structural body of the A-sandwich type. It is approximately 4" thick and the 9 sub-sections are assembled into a continuous weather protective roof (Figure 6).

Four flood lamps directed toward the radome provide uniform chamber lighting. The lamps are located at the four upper corners of the chamber such that they are well hidden by the absorber on the walls. As a result, the lighting is uniform and avoids the visual problem of looking into the lamps; there is a minimum of RF reflection from the fixtures since they are well shadowed by the 70" absorbent material.

Finally, the chamber is temperature-controlled to prevent large variations of temperature which may affect antenna measurements.

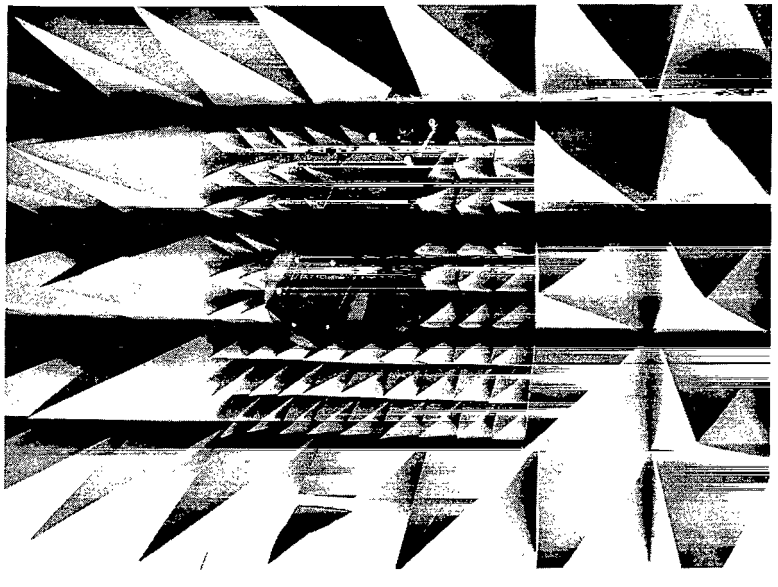

Figure 4—Photograph of wall mounting for satellite antenna in anechoic chamber.

Figure 5—Photograph illustrating size of absorbent material.

Figure 6—Photograph of nine-panel radome.

Electrical Description

Electrically the chamber was lined on 5 surfaces with commercially-supplied RF absorbent material and the 6th side enclosed by an RF transparent radome.

Each piece of the absorbent material is a 70" high pyramid with a 2-foot square base. All absorbent material exhibits a minimum reflection coefficient of 28 db at 120 Mc, 40 db at 400 Mc and 50 db from 1,000 to 10,000 Mc.

The reflection coefficient tests on the absorber were made with a closed loop technique at 120 Mc and 400 Mc. At 1,000, 5,000 and 10,000 Mc an open loop technique was used. The closed loop technique consisted of measuring four 2'×2' pyramidal foam absorbers at a time in a flared waveguide system in which the absorbent material served as a test load. The absorber was moved inside the waveguide and the resulting standing wave moved in conjunction with the physical movement of the absorber. A fixed probe inside the waveguide (located between the absorber and RF oscillator) detected the standing wave and suitable instruments were used to make a reflected power measurement.

The open loop testing technique consisted of a horizontal version of the Naval Research Laboratory arch method. A flat 2'×8' metal plate was used as a reflecting surface. The reflection levels of four 2'×2' pyramidal foam absorbers were measured and compared to the flat metal plate. The reflectivity of the absorbent material was taken as the difference in return power in db between the metal plate and the absorbent material.

The radome was supplied commercially. The electrical characteristics of the A-sandwich radome material were specified as follows:

(a) Transmission loss $\leq$ 7.5% over the frequency range 120 Mc to 10,000 Mc.
(b) Refraction less than 10% for angles of incidence from 0° to 45°.
(c) Loss tangent of glass laminate = .005.
(d) Dielectric constant of glass laminate = 4.0.
(e) Loss tangent of foam core = .0005.
(f) Dielectric constant of foam core = 1.12.

Although manufacturer's tests confirm the specifications on a flat 40"×40" sample of the radome, measurements indicate that the actual radome does exhibit less than specified performance particularly at frequencies above 1,000 Mc. This can be easily explained since the actual completed radome has a curved surface and the nine pieces comprising the total radome are assembled with beefed-up glass laminate flange sections. These two conditions increase the detrimental diffraction and reflection effects.

The frequencies of primary interest were in the 120 Mc to 400 Mc region, but some tests were performed at higher frequencies in order to evaluate chamber characteristics.

Normally, in evaluating the chamber a quiet zone is defined. That is, a volume within the chamber in which known (measured) reflectivity levels exist. Within this zone antenna systems can then be comprehensively evaluated and the limitations of the chamber taken into account. The quiet zone is, by definition, a sphere which is tangent to the walls, floor and ceiling of a chamber of cubical working dimensions (14'×14'×14'). If one dimension is reduced (14'×14'×10') then the diameter of the sphere is reduced (from 14' to 10').

Advantages

Ground reflections are the most serious source of error when using a conventional test range for measurements of low-frequency low-gain antennas. The error may be reduced to a degree by additional tower height but towers over 100' high are expensive and rather inconvenient to use. Likewise, a conventional anechoic chamber designed for operation at low frequencies is expensive and requires a large building to provide even a modest size test range. The vertical test range provides an attractive compromise between tall towers and a large anechoic chamber. The chamber portion need only be large enough to prevent reflections from the ground and nearby reflecting surfaces and the tower need only be tall enough to hold an antenna out of the near field of the antenna under test. Furthermore, the length of the test range may easily be varied by adjusting the

height of the outside antenna. Operation of a vertical range is especially convenient; since the model under test, the test and control equipment, and personnel are all at ground level and the need for hoists and elevators is eliminated.

ANALYSIS OF CHAMBER

The magnitude of unwanted reflections that can be tolerated in an antenna test range has been shown to be a function of the parameter being measured. Since the site is never perfect, the results obtained may be interpreted in terms of the known site imperfections, provided the reflection coefficients and (in some cases) phase are accurately specified. However, measurement of the reflection coefficient of absorbent materiels is difficult and techniques for its evaluation have not been standardized. Currently the pattern comparison technique and the free space VSWR technique* are favored in evaluation of RF anechoic chambers. In both techniques the significant result is the comparison of the incident to the reflected energy from an absorbing wall to determine its reflection coefficient.

Briefly, in the pattern comparison technique, the pattern of a high-gain directive antenna is measured successively at closely spaced points along the radii of the chamber quiet zone (previously defined). Then the patterns are superimposed on each other with pattern peaks coincident. The deviations in the patterns are read at different aspect angles, and VSWR curves vs aspect angle are constructed. The curves may then be converted to reflection levels within the chamber.

The free space VSWR technique is a method of continuously recording the amplitude variations produced by reflections. Two directive antennas are used, one being moved continuously across the chamber quiet zone at a discrete aspect angle for each recording. The recorded amplitudes are reduced to incident and reflected energy levels, thus allowing the reflection coefficient vs aspect angle of a chamber to be determined.

From the brief summary above (References 1 to 4) it can be seen that both techniques rely on the use of directive antennas. This is not a disadvantage in the usual situation, where the chamber is large in terms of wavelength, and directive antennas are usually evaluated. However, in the vertical test range more emphasis is placed on measurement of nearly omnidirectional antennas in a termination chamber that is electrically small ($1\lambda \times 2\lambda \times 2\lambda$). Although evaluation of chamber performance using directive antennas will indicate both a direction and reflection coefficient for sources of reflections; unless considerable effort is made to integrate the reflection levels from all directions the chamber will appear better than when used with an omnidirectional antenna. Therefore most of the analysis of both the scale model and the full scale range was made using a dipole antenna to probe the energy levels within the termination chamber. In this method, a dipole antenna was moved throughout the quiet zone and energy levels vs position were recorded. The difference between the recorded levels and the calculated free space levels were converted into VSWR values and finally a reflection coefficient was computed.

*Emerson, W., "Chamber Information," unpublished anechoic chamber design data report of B. F. Goodrich Company, Shelton, Conn.

It is common practice to try to reduce the large number of different reflection coefficients that are measured in evaluating a chamber to a single value defining the chamber's performance. In general, it will be found that this value does not accurately describe a chamber, and that the relative performance of two different chambers should not be judged on a single defining value. For instance, the quiet zone of chamber A may be only 1/3 of the volume that was included in evaluation of chamber B; yet chamber B may be considerably better than A over the same quiet zone. Unfortunately, the performance rating of anechoic chambers is like the evaluation of radio receivers in 1940, i. e., not complete unless the test conditions are known as well as the results.

Scaled Chamber Measurements

Reflection coefficient measurements were made in a 1/9th-scale anechoic chamber. A photograph of the scale chamber is shown in Figure 7. Figure 8 defines the test set-up. No attempt was made to design and test a 1/9th-scale radome because the radome would appear as a thin-wall structure at the frequencies of most interest (up to around 400 Mc) in the full scale chamber. Although no scaled radome measurements were made in this particular chamber design it is felt that general comments on scaled radome measurements are in order.

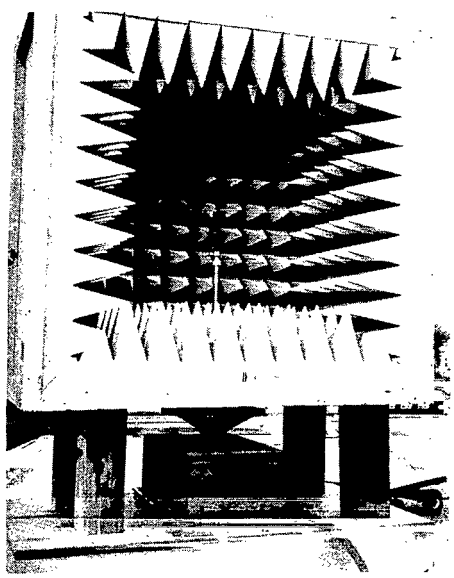

Figure 7—Photograph of 1/9th-scale anechoic chamber.

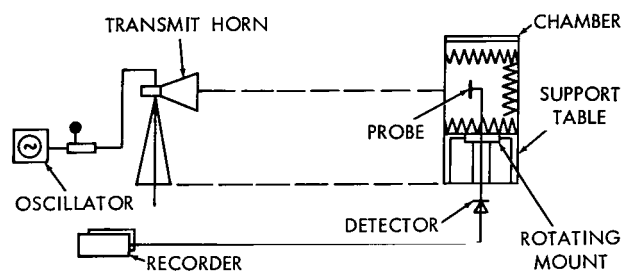

Figure 8—Test equipment setup for 1/9th-scale anechoic chamber measurements.

Scaling a multi-panel, sandwich radome is, in general, difficult. Extreme care must be taken in scaling the ribbing, flange design and radome curvature. Serious errors can be expected if this precaution is not taken. Thin wall structural radomes of dielectric constants of approximately 3 or 4 may be scaled for measurements with confidence and also thick wall foam radomes of low dielectric constants $(\epsilon_n = 1.1 \text{ to } 1.4)$ are practical for scaling purposes.

Measurements were made at frequencies from near 1,080 Mc to 3,600 Mc. This corresponds to full scale chamber measurement of approximately 120 Mc to 400 Mc. A dipole probe is used inside the scaled chamber to prevent discrimination against any reflected energy, as a directive antenna would have been too selective.

The measurements at 1,080 Mc in the 1/9th-scale chamber indicated a reflection coefficient of 20 db, and at 3,600 Mc a reflection coefficient of 30 db.

Figure 9 is typical of the standing waves measured by probing the scaled chamber with dipoles. The dipole probes were moved in small increments in terms of wavelengths from the aperture of the chamber to the back. Figure 10 depicts standing wave curves resulting from probing across the chamber in small increments. These data are typical of that obtained in the 1/9th-scale chamber, and it was from these measurements that the full-scale chamber performance was predicted.

As was mentioned previously, no attempt was made to determine the effect of an A-sandwich type radome on the full scale chamber at scaled frequencies. That the radome effect would be negligible at the low frequencies of interest was predicted on the basis that the radome would appear as a thin wall (approximately $\lambda/8$ thick or less) below 400 Mc.

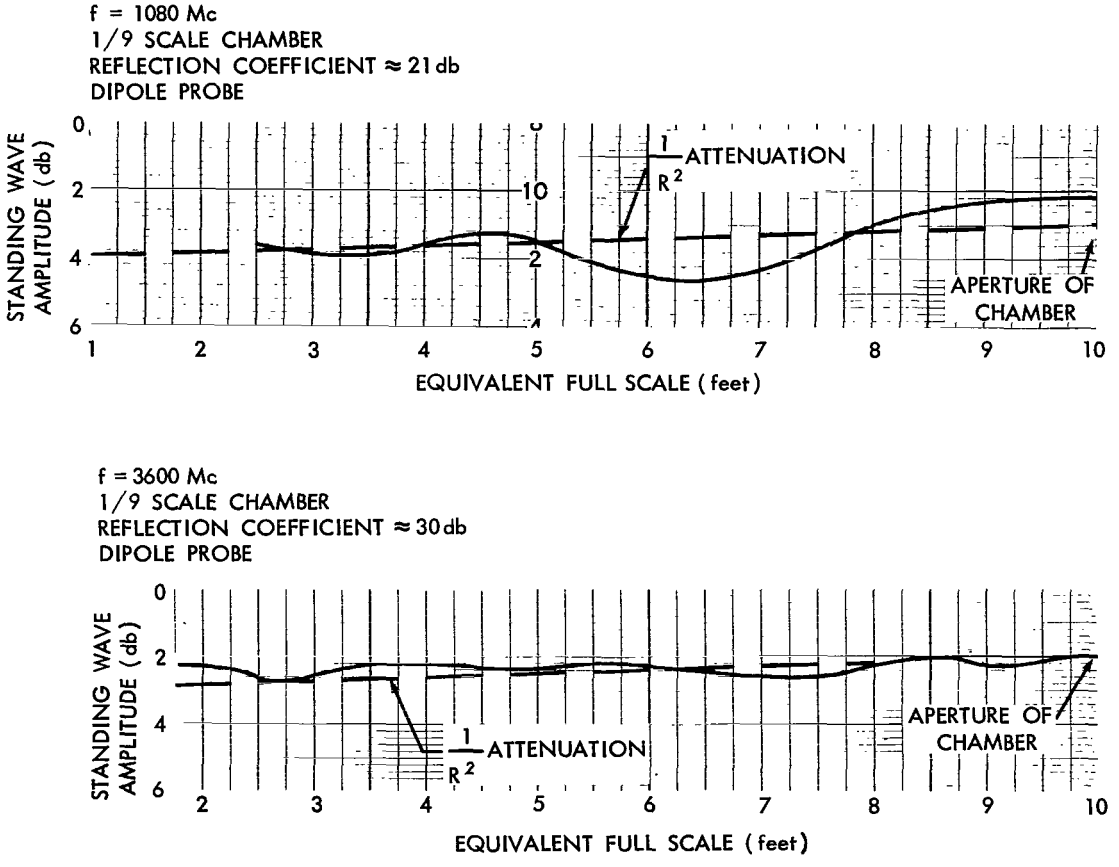

Figure 9—Plots of standing waves in 1/9th-scale anechoic chamber, measured from aperture of chamber to floor.

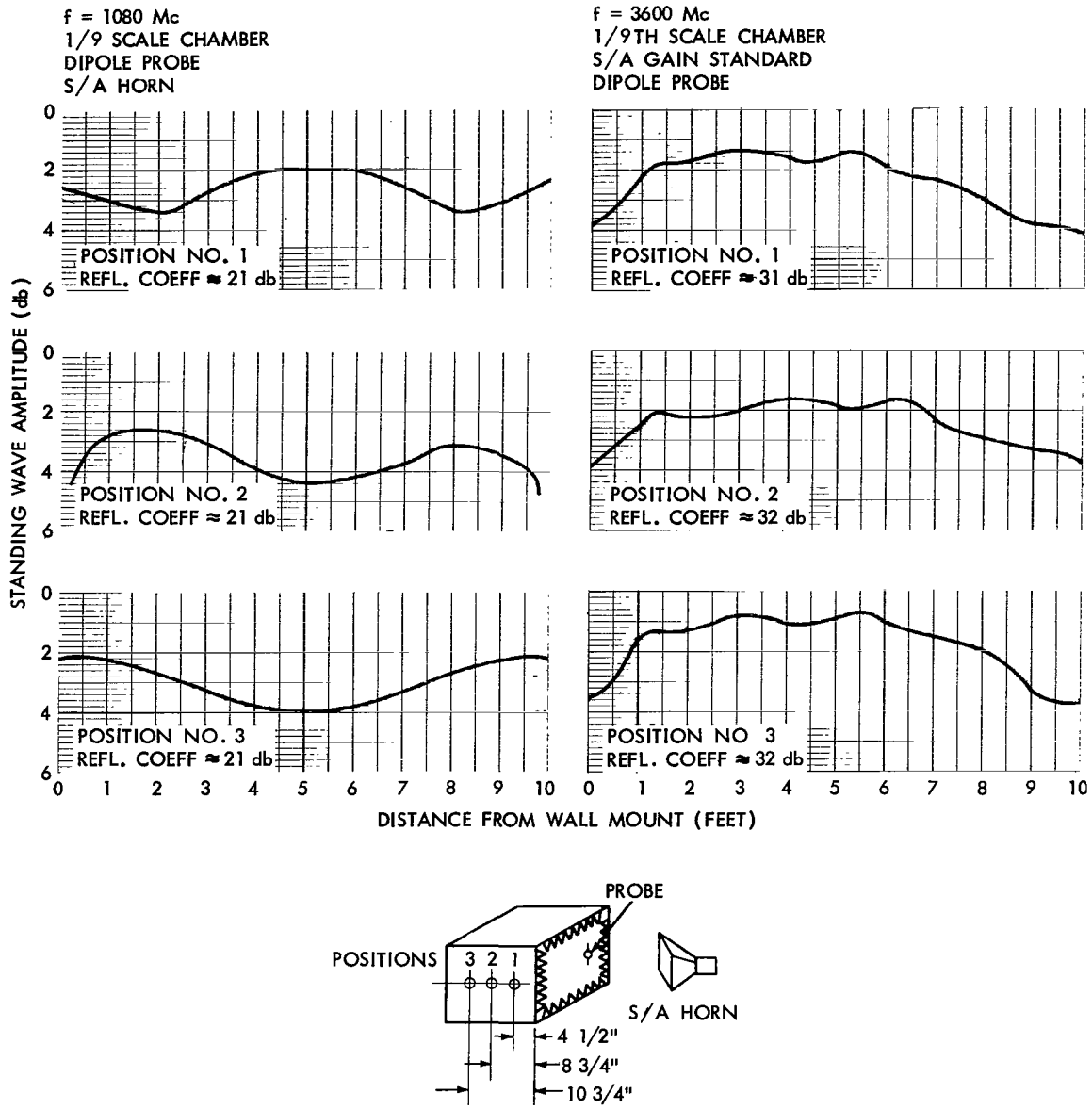

Figure 10—Plots of standing waves in 1/9th-scale anechoic chamber, measured across aperture.

Full Scale Chamber Measurements

The quiet zone of the chamber was probed with a dipole using an illuminating antenna which was directional in nature. At 125 Mc and 400 Mc the magnitude of the reflection coefficient was determined by moving a dipole horizontally inside the chamber in directions normal to each wall and across the diagonals. With the dipole fixed to a cart made of low dielectric constant foam material, the cart was moved along tracks which could be oriented as desired within the chamber. The track, cart and dipole support are shown in Figure 11. Three horizontal measurements were made at discrete heights of 2 (and/or 3), 4, 5, 6 and 8 feet above the floor of the chamber. The reflection coefficient in the vertical direction was determined by measuring the standing wave as

Figure 11—Photograph of track and cart arrangement for reflection coefficient measurements.

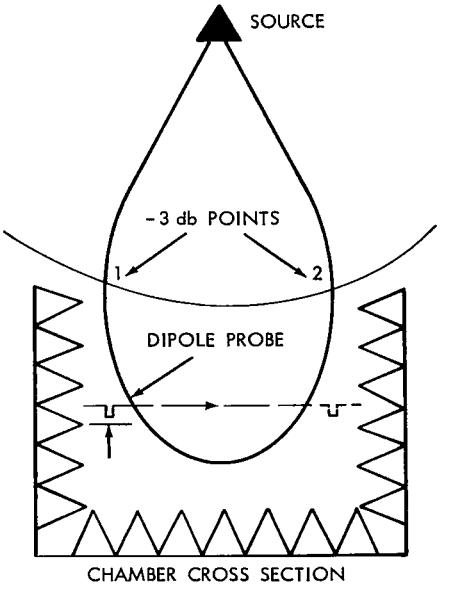

(a)

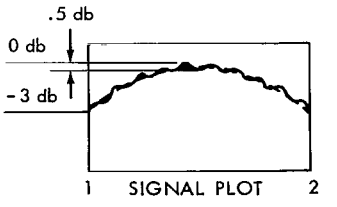

(b)

Figure 12—Interpretation of standing wave plots for measurements across aperture.

a function of vertical movement of the dipole. The resultant standing wave curves are converted to an equivalent reflected energy level (reflection coefficient). Figure 12 is a typical plot, where the dashed curve represents the probed energy level as measured in the absence of reflected energy, and the solid curve represents the effect of the probed energy level along with reflected energy. The peak-to-peak value of the standing wave is 0.5 db, and it results from a reflected energy level of 30 db below the incident signal level, where the reflection coefficient = 20 log [(VSWR-1)/(VSWR+1)]. Measured curves are shown in Figures 13 through 16.

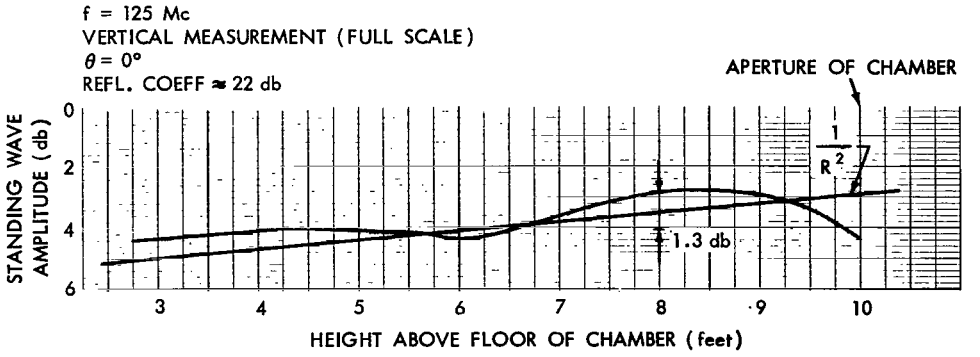

Figure 13—Full-scale measurements of standing waves at 125 Mc. (Vertical Direction)

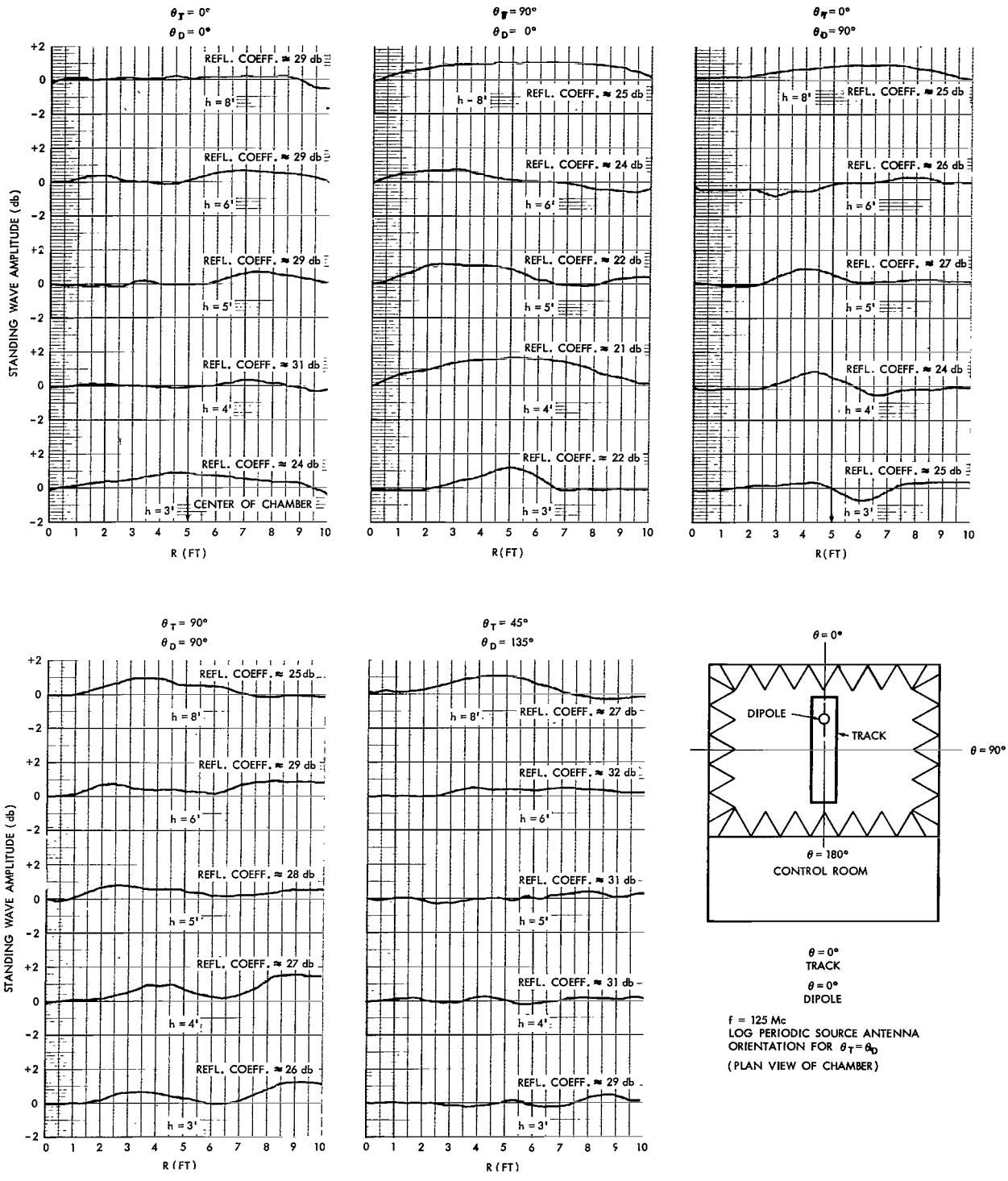

Figure 14—Full-scale standing wave plots at 125 Mc. (Horizontal Direction)

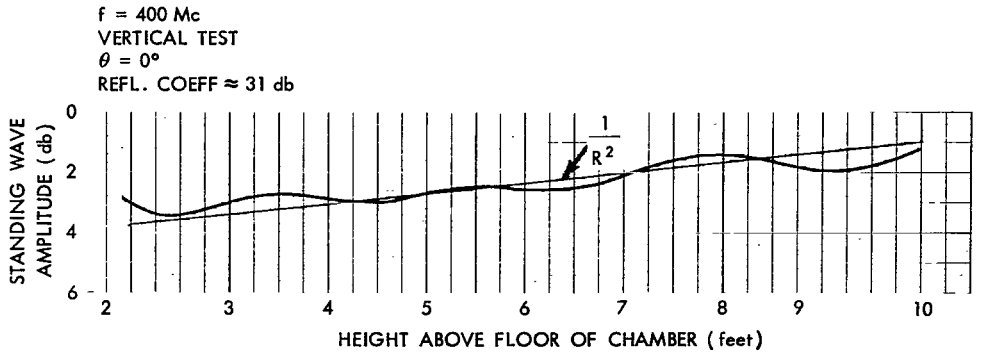

Figure 15—Full-scale measurements of standing waves at 400 Mc. (Vertical Direction)

At 1,200 Mc the reflected energy levels were greater than expected (approximately 32 db average), and the reflected energy levels were polarization-sensitive (i. e., E-perpendicular vs E-parallel) with differences in reflection coefficients between 6 and 15 db as a function of aspect angle. This deviation from the anticipated levels of 45 to 50 db was attributed to the radome for two reasons: (1) the chamber at 1,200 Mc is electrically large ($15\lambda \times 15\lambda$ 10λ) and therefore the chamber would be expected to be much better than at 400 Mc (reflection levels $\approx$ 32 db); and (2) this A-sandwich radome (4 inches thick, with solid fiberglass panel flanges) appears as a relatively large discontinuity.

Measured magnitudes of reflected energy at 125 Mc and 400 Mc for various linear polarization orientations are tabulated in Tables 1 and 2. Some inconsistency is apparent, especially in the higher coefficient values measured at 125 Mc. This is attributed to instability of the measurement equipment; however, retests of selected orientations indicate no serious differences from the data presented or the conclusions drawn from the data.

Table 1

125 Mc Chamber Reflectivity Levels

Track Orientation θ_T	Dipole Orientation θ_D	Reflection Coefficient (db)				
		h = 3 ft	h = 4 ft	h = 5 ft	h = 6 ft	h = 8 ft
0°	0°	24	31	29	29	29
0°	90°	25	24	27	26	25
90°	0°	*27	*26	*28	*24	*20
90°	90°	26	27	28	29	25
45°	45°	29	22	24	23	*25
45°	135°	29	31	31	32	27
135°	45°	26	21	21	21	22
135°	135°	*22	*21	*24	*24	*21

*Measurements performed at 123 Mc using NASA battery operated signal generator.

Table 2

400 Mc Chamber Reflectivity Levels

Track Orientation θ_T	Dipole Orientation θ_D	Reflection Coefficient (db)				
		h = 2 ft	h = 4 ft	h = 5 ft	h = 6 ft	h = 8 ft
0°	0°	31	39	31	35	32
0°	90°	39	39	31	32	31
90°	0°	31	32	32	31	30
90°	90°	31	32	32	32	31
45°	45°	31	39	39	34	32
45°	135°	32	31	30	31	32
135°	45°	35	32	31	35	30
135°	135°	32	32	30	31	39

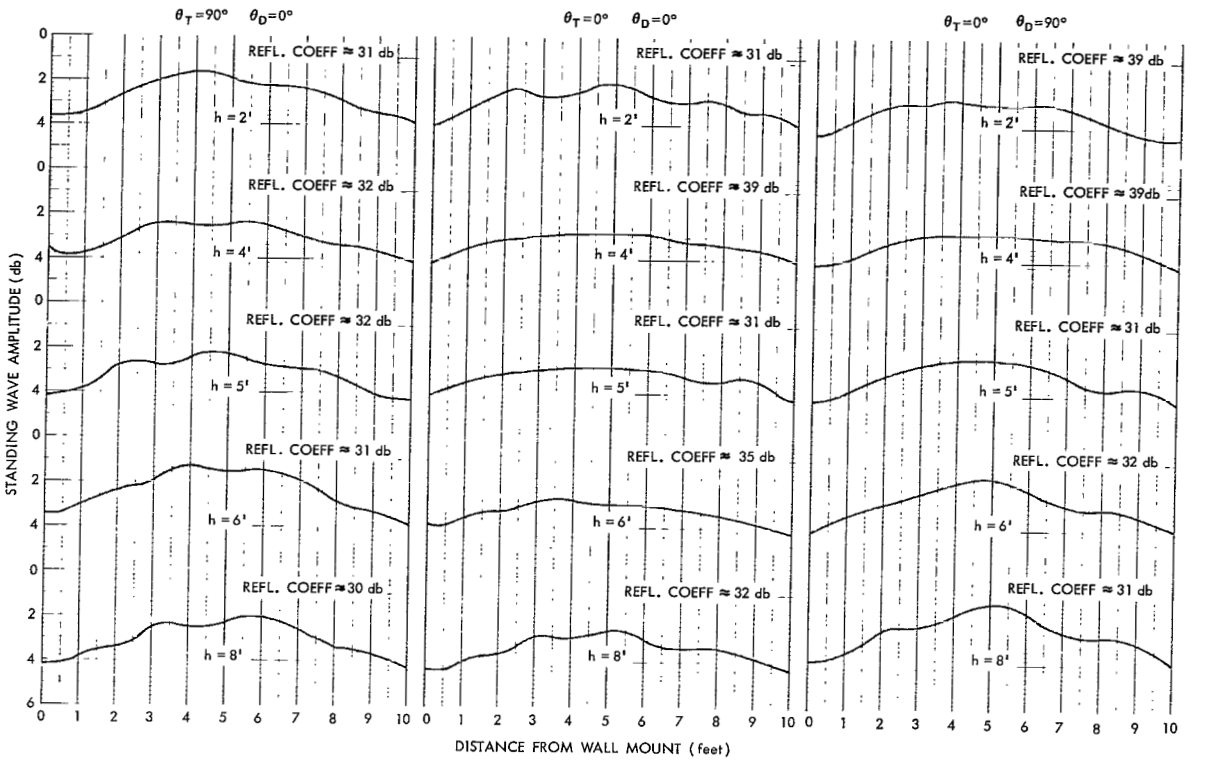

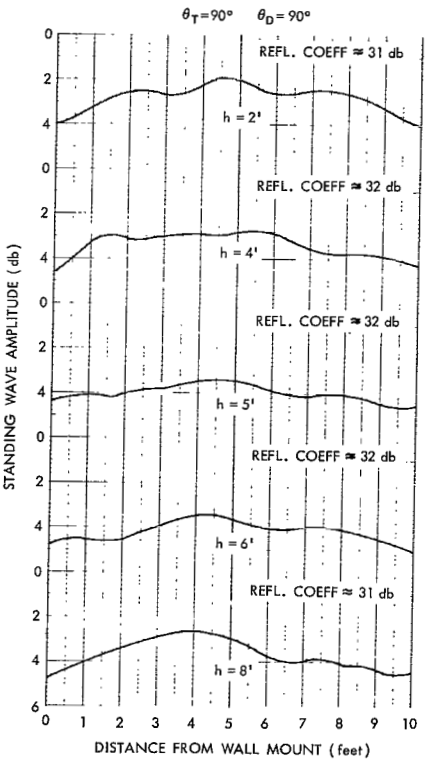

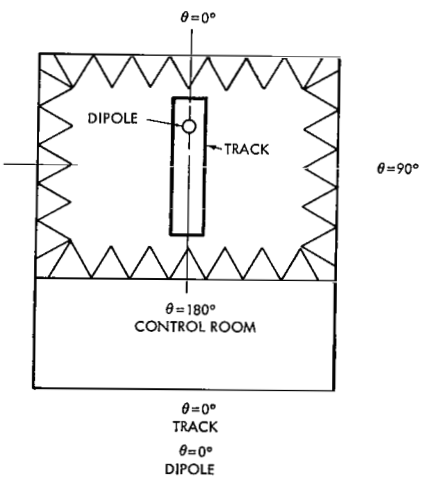

f=400 mc
LOG PERIODIC SOURCE ANTENNA
ORIENTATION FOR $\theta_T = \theta_D$
(PLAN VIEW OF CHAMBER)

Figure 16—Full-scale standing wave plots at 400 Mc. (Horizontal Direction)

Data taken at 1,200 Mc are not presented because later tests prove that the radome is the major contributor to standing waves within the chamber and therefore does not truly represent the capability of a vertical test range.

To verify the fact that the radome caused larger than anticipated reflection coefficients and polarization sensitivity, measurements were performed with the source antenna inside the chamber just under the radome, and compared to the pattern taken through the radome (Figure 17a). Thus, an interference pattern (see Figure 17b) between incident and reflected energy was produced by essentially removing the radome from between the source and receive antenna. In both cases a horn antenna was moved across the chamber at an angle of 45° from the vertical. A value of +45° refers to the horn antenna being tilted toward the chamber wall containing the wall mount, and a value of −45° refers to an angle toward the wall without the wall mount.

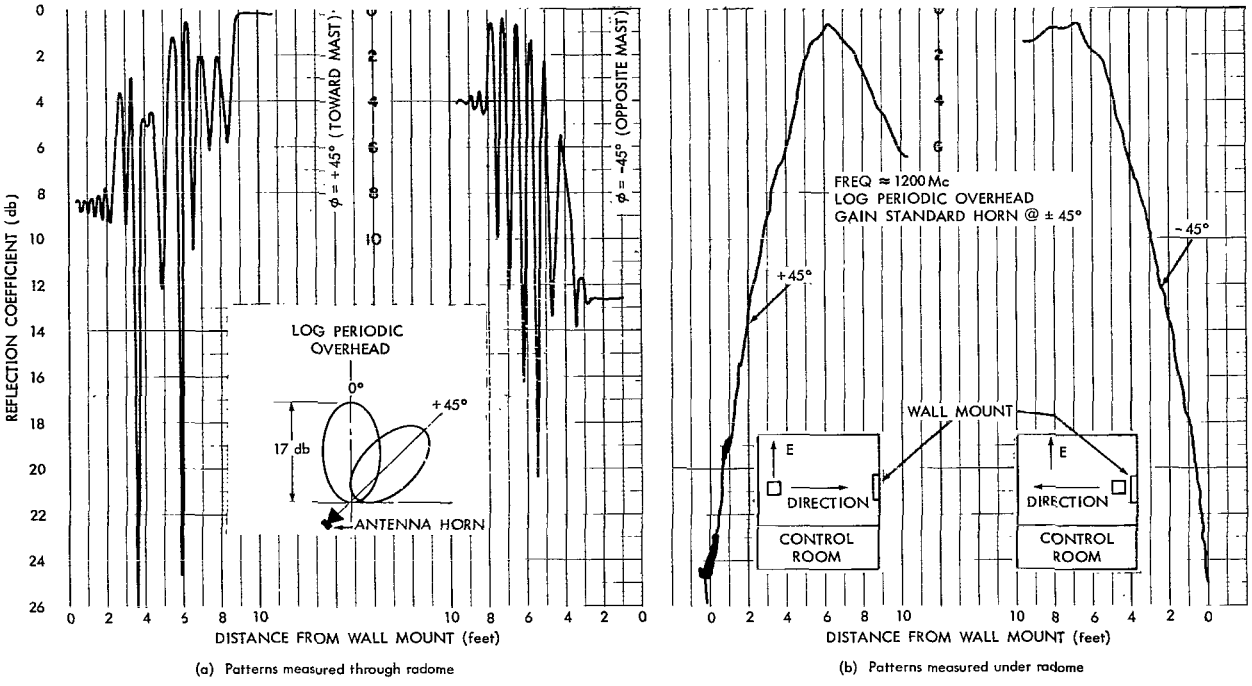

Figure 17—Radiation plots showing effect of radome on reflection coefficient at 1200 Mc.

Except at angles far from normal incidence, reflected energy from E-perpendicular is nearly always greater than from E-parallel because of the zero Brewster angle occurring only with parallel polarization (Figure 18). From Figure 19 it can be seen that the difference in reflection coefficients is 14 db. The Brewster angle (where the reflection value goes to zero) is defined as follows:

$$\theta_B = \tan^{-1} \sqrt{\frac{\epsilon_2}{\epsilon_1}} \text{ where } \epsilon_2 > \epsilon_1 \ . \qquad (11)$$

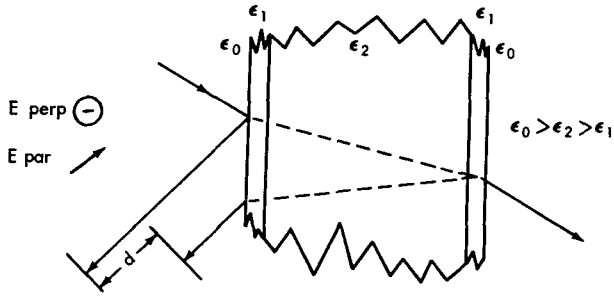

Figure 18—Reflected energy in the E-parallel and E-perpendicular polarization modes.

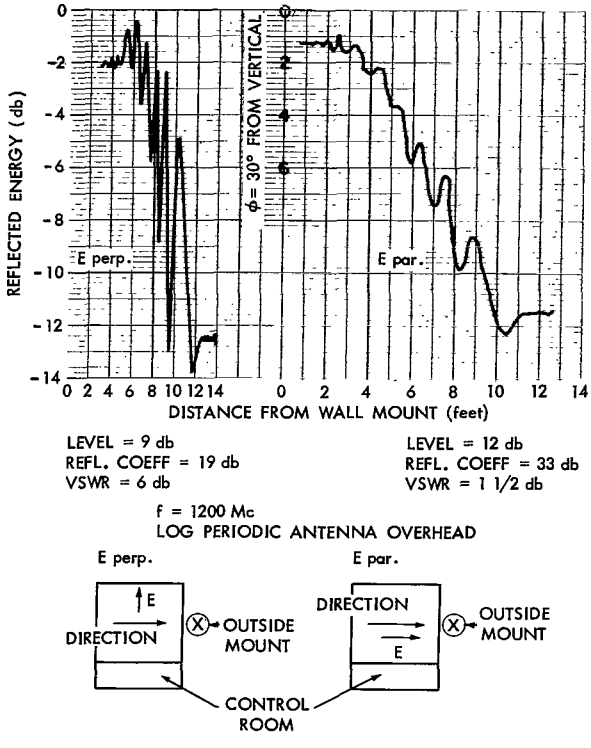

Figure 19—Effect of radome on parallel and perpendicular polarization.

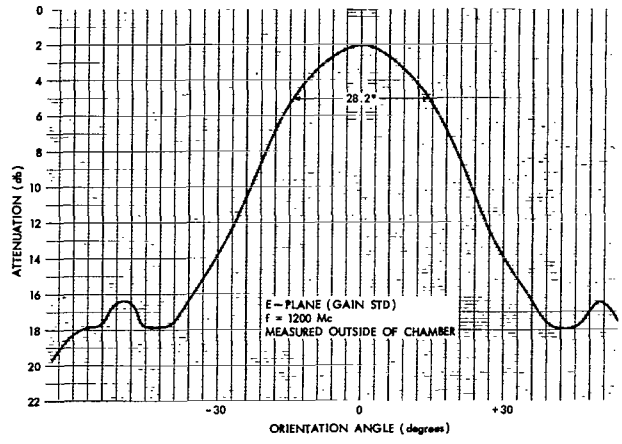

Figure 20—Pattern of E-plane horn antenna measured outside chamber at 1200 Mc.

Plots in Figure 19 compare the standing waves of the A-sandwich radome for the E-parallel and E-perpendicular polarization modes.

An important point that is illustrated in Figures 20 and 21 is the degree of accuracy with which the antenna radiation pattern can be measured through a radome exhibiting significant reflection characteristics. Here the standard antenna radiation pattern was measured at 1200 Mc first by a free space pattern range method, and then the measurement was repeated inside the vertical chamber. To measure the pattern inside the chamber, the antenna was rotated about a fixed axis and not moved across the chamber. Therefore, the "available" reflections which exist are not examined and a rather respectable pattern can be achieved. Figure 21 also shows the effect that the wall mount can produce in terms of reflected energy.

CONCLUSIONS

Measurements taken from the 1/9th-scale model of the test range are in reasonable agreement with the measurements of the full-scale range. The structural A-sandwich radome definitely reduces the performance of the facility at higher frequencies, but does not affect operation in the frequency range of primary interest (125–400 Mc).

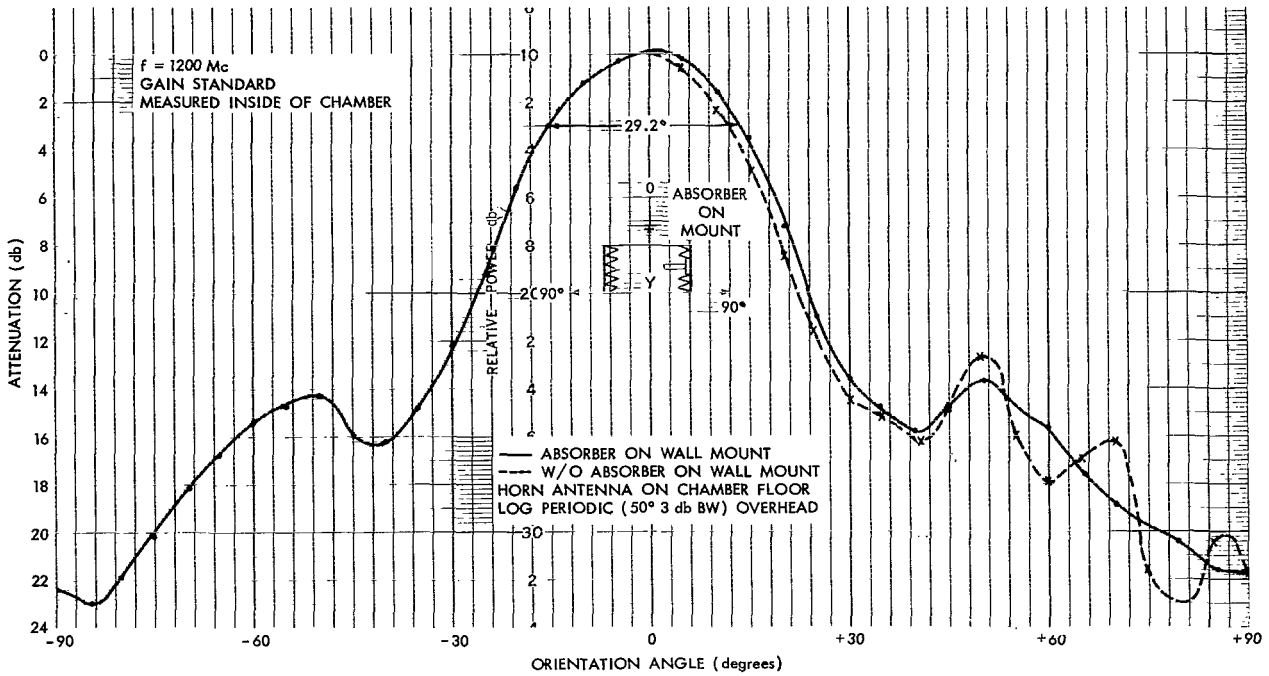

Figure 21—Pattern of E-plane horn antenna measured inside chamber at 1200 Mc.

The concept of a vertical test range composed of an electrically small termination chamber with a RF transparent radome has been found feasible, and provides a convenient, quasi-all-weather, facility for accurate measurement of antenna characteristics at moderate cost.

RECOMMENDATIONS

Considerable confidence may be placed on the results of measuring scale models of anechoic chambers. Since the instrumentation is not difficult and the cost is small it is recommended that more extensive use be made of scale models to check chamber and anechoic material performance.

A multipanel sandwich radome has definite frequency limitations when used as part of an antenna test range. Therefore it is recommended that a thick, low-dielectric-constant foam radome be used.

(Manuscript received October 13, 1964)

REFERENCES

1. Buckley, E. F., "Outline of Evaluation Procedures for Microwave Anechoic Chamber," *Microwave Journal* 6(8):69-75, August 1963.

2. Jasik, H., editor, "Antenna Engineering Handbook," 1st Edition, New York: McGraw-Hill Company, 1961.

3. Harvey, A. F., "Microwave Engineering," New York: Academic Press, 1963.

4. Vitale, J. A., Cohen, A., Davis, P., Nilo, S. C., D'Amato, R., and Maltese, A. W., "Ground Radomes: Performance, Economics, Histroy, Types," West Concord, Mass: Electronic Space Structures Corp., Jan. 31, 1964.

"The aeronautical and space activities of the United States shall be conducted so as to contribute . . . to the expansion of human knowledge of phenomena in the atmosphere and space. The Administration shall provide for the widest practicable and appropriate dissemination of information concerning its activities and the results thereof."

—NATIONAL AERONAUTICS AND SPACE ACT OF 1958

NASA SCIENTIFIC AND TECHNICAL PUBLICATIONS

TECHNICAL REPORTS: Scientific and technical information considered important, complete, and a lasting contribution to existing knowledge.

TECHNICAL NOTES: Information less broad in scope but nevertheless of importance as a contribution to existing knowledge.

TECHNICAL MEMORANDUMS: Information receiving limited distribution because of preliminary data, security classification, or other reasons.

CONTRACTOR REPORTS: Technical information generated in connection with a NASA contract or grant and released under NASA auspices.

TECHNICAL TRANSLATIONS: Information published in a foreign language considered to merit NASA distribution in English.

TECHNICAL REPRINTS: Information derived from NASA activities and initially published in the form of journal articles.

SPECIAL PUBLICATIONS: Information derived from or of value to NASA activities but not necessarily reporting the results of individual NASA-programmed scientific efforts. Publications include conference proceedings, monographs, data compilations, handbooks, sourcebooks, and special bibliographies.

Details on the availability of these publications may be obtained from:

SCIENTIFIC AND TECHNICAL INFORMATION DIVISION

NATIONAL AERONAUTICS AND SPACE ADMINISTRATION

Washington, D.C. 20546